

Submitted to the *Astrophysical Journal Letters*

Contribution to Unresolved Infrared Fluctuations from Dwarf Galaxies at Redshifts of 2 – 3

Ranga-Ram Chary¹, Asantha Cooray², Ian Sullivan¹

ABSTRACT

In order to understand the origin of clustered anisotropies detected in *Spitzer* IRAC images, we stack the *Spitzer* IRAC/Great Observatories Origins Deep Survey (GOODS) images at pixel locations corresponding to faint, $m_{AB}(\text{z-band}) \sim 27$ mag, optical sources with no obvious IR counterparts. We obtain a stacked median flux of 130 ± 5 nJy at $3.6\mu\text{m}$. We also use the wealth of multi-wavelength data in GOODS to measure the stacked spectrum of these sources from the ultraviolet to near-infrared bands. The median flux spectrum is consistent with a $L \lesssim 0.03 L_{*,\text{UV}}$ galaxy population at $z \sim 2.5$. They produce a $3.6\mu\text{m}$ absolute background intensity between 0.1 and $0.35 \text{ nW m}^{-2} \text{ sr}^{-1}$ and the clustered IR light could account for $\sim 30 - 50\%$ of fluctuation power in the IR background at 4 arcminute angular scales. Although the redshift distribution of these sources is unknown, they appear to contain between 5 – 20% of the co-moving stellar mass density at $z \sim 2.5$.

Subject headings: large scale structure of universe — diffuse radiation — infrared: galaxies

1. Introduction

The intensity of the cosmic near-infrared background (IRB) is a measure of the total light emitted by stars and galaxies in the universe which is not thermally reprocessed by dust. While the absolute background has been estimated with the Diffuse Infrared Background

¹Division of Physics, Mathematics, and Astronomy, California Institute of Technology, Pasadena, CA 91125. Email: rchary@caltech.edu

²Center for Cosmology, Department of Physics and Astronomy, University of California, Irvine, CA 92697. E-mail: acooray@uci.edu

Experiment (DIRBE; Hauser & Dwek 2001) and the Infra-Red Telescope in Space (IRTS; Matsumoto et al. 2005), there are still large uncertainties associated with the removal of foreground zodiacal light (Dwek et al. 2005). Still, attempts have been made to explain the difference between measured and resolved IRB intensity with sources during reionization (e.g., Santos, Bromm & Kamionkowski 2002; Salvaterra & Ferrara 2003; Cooray & Yoshida 2004; Fernandez & Komatsu 2006). If first-light galaxies are to explain the missing intensity completely, then an extreme scenario is needed with the conversion of more than 10% of baryons to stars (Madau & Silk 2004). Indirect limits from TeV blazar spectra, however, suggest that the total IRB light intensity is smaller than estimated directly (Aharonian et al. 2005) and $\sim 90\%$ of the IRB light is from known galaxy populations.

Instead of the absolute intensity, recent works have concentrated on spatial fluctuations of the IRB (Cooray et al. 2004; Kashlinsky et al. 2004). While an interpretation of unresolved fluctuations is subject to extremely uncertain astrophysical modeling of underlying faint populations, fluctuations in deep *Spitzer* images have been attributed to first-light galaxies containing Pop III stars during reionization (Kashlinsky et al. 2005). The same fluctuations can be alternatively explained with clustering of faint, unresolved sources at lower redshifts (Sullivan et al. 2007; Cooray et al. 2007). Thus, while two independent studies find a similar clustering amplitude for IRB fluctuations (Kashlinsky et al. 2004; Cooray et al. 2007), they differ in their interpretation due to differences in the background light ascribed to faint foreground galaxies unresolved by *Spitzer*.

The suggestion for a low redshift origin in Cooray et al. (2007) comes from predictions using a halo model (Cooray & Sheth 2002) for the $3.6\text{ }\mu\text{m}$ population matched to their luminosity functions (Babbedge et al. 2006) and clustering spectra (Sullivan et al. 2007). In Cooray et al. (2007) this low-redshift population was identified as the faint optical galaxies that are resolved in the *Hubble* Advanced Camera for Surveys (ACS; Giavalisco et al. 2004) images of the Great Observatories Origins Deep Survey (GOODS; Dickinson et al. 2003) fields, but not detected in deep *Spitzer* Infrared Array Camera (IRAC) images of the same fields. With models, it was estimated that this faint galaxy population has a $3.6\text{ }\mu\text{m}$ intensity between 0.1 and $0.8\text{ nW m}^{-2}\text{ sr}^{-1}$. The analysis in Cooray et al. (2007) did not exclude a high redshift contribution to the IRB, with an upper limit on the $3.6\text{ }\mu\text{m}$ absolute background intensity from $z > 8$ sources of $0.6\text{ nW m}^{-2}\text{ sr}^{-1}$. In comparison, if all unresolved IR fluctuations are generated by $z > 8$ sources, then the IRB intensity for such sources is between 2 and $4\text{ nW m}^{-2}\text{ sr}^{-1}$ at $3.6\text{ }\mu\text{m}$ (Kashlinsky et al. 2007).

In this *Letter*, we further study the physical origin of fluctuations in the IR background. Since faint ACS optical sources are undetected in deep *Spitzer* IRAC images, we stack their pixel locations in IRAC to establish the average IR flux. We also utilize the wealth of

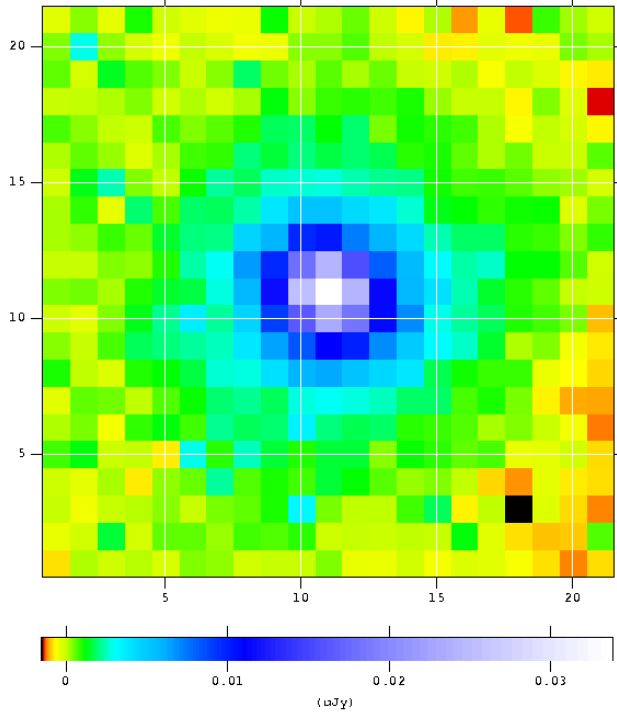


Fig. 1.— The average-stacked $3.6 \mu\text{m}$ image from GOODS-N with pixel locations of all 6160 ACS sources unmatched and unmasked in IRAC. The median stacked flux is (130 ± 5) nJy (or $= 26.1 \pm 0.1$ magnitude) and is detected with a statistical signal-to-noise ratio higher than 25.

multiwavelength imaging data in the GOODS fields to obtain a stacked broadband spectral energy distribution of these faint optical galaxies between UV and near-IR bands. We identify the average optical to IR flux spectrum to be a $\sim 0.03 L_{*,\text{UV}}$ galaxy at $z \sim 2.5$, similar to a scaled-down population of Lyman-break galaxies. We also measure the expected IRB fluctuation clustering spectrum from these sources.

The *Letter* is organized as following: in the next section, we summarize the stacking analysis and discuss results on the average optical to IR flux spectrum in § 3. We discuss clustering of these faint optical sources in § 4. In § 5 we discuss implications of our measurements. The magnitudes quoted throughout this paper are AB magnitudes.

Table 1. Results from Stacking Analysis

	GOODS-N	GOODS-S
$\Delta\Omega/\text{arcmin}^2$	169	171
N_{ACS}	6160	5441
U	28.3 ± 0.1	28.4 ± 0.1
B	28.0 ± 0.1	27.8 ± 0.1
V	27.5 ± 0.1	27.4 ± 0.1
i	27.2 ± 0.1	27.1 ± 0.1
z	27.1 ± 0.1	27.0 ± 0.1
HK'	27.3 ± 0.3	...
J	...	26.9 ± 0.15
H	...	26.7 ± 0.15
Ks	...	26.6 ± 0.15
$3.6 \mu\text{m}$	26.1 ± 0.1	26.0 ± 0.1
$4.5 \mu\text{m}$	26.2 ± 0.1	26.2 ± 0.1
$5.8 \mu\text{m}$	26.2 ± 0.1	26.0 ± 0.1
$8.0 \mu\text{m}$	26.3 ± 0.15	26.0 ± 0.15

Note. — N_{ACS} is the total number of faint ACS sources over an effective area $\Delta\Omega$ that were included in the stack. Uncertainties in the stacked flux (tabulated in AB magnitudes) are mostly dominated by calibration systematics.

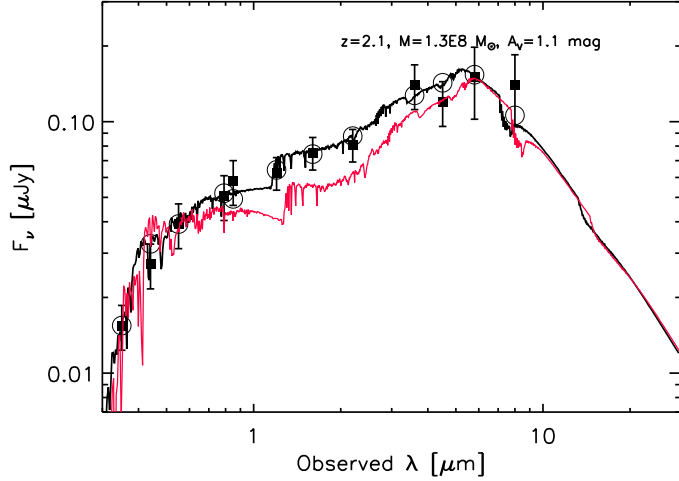


Fig. 2.— The stacked ultraviolet to IR flux spectrum of faint galaxies detected by ACS but not detected individually by *Spitzer*/IRAC in GOODS-S (black line and data points). The spectrum is consistent with the sub- $L_{*,\text{UV}}$ galaxy population at $z \sim 2.5$. The parameters of the stacked galaxy for GOODS-S are as shown in the legend. The stacking in GOODS-N results in a best fit redshift of $z \sim 2.6$ and the SED shown as the red line.

2. Stacking Analysis

To establish the average IR intensity of faint optical sources that are unresolved in *Spitzer* IRAC images we stack the IRAC images at the spatial coordinates of sources which are ACS detections. The stacking begins by first masking all $> 3\sigma$ detected IRAC sources with $m_{\text{AB}}(3.6\mu\text{m}) < 26.7$ mag. This limit is fainter than the 50% completeness limit of 24.7 mag. The mask has a radius of $13.5''$ for a source with 18 mag and scales linearly with magnitude down to $2.4''$ for sources fainter than 22 mag. We then identified sources in the GOODS ACS catalogs (Giavalisco et al. 2004) which are in unmasked regions of the IRAC image and are therefore IRAC undetected. While there are close to 22,000 ACS sources which are unmatched with IRAC sources to within $\sim 0.5''$, only 6,160 (GOODS-N) and 5,441 (GOODS-S) sources are sufficiently separated from brighter IRAC sources so as to be in unmasked regions of the IRAC image. The IRAC images were stacked at the pixel locations corresponding to these ~ 6000 ACS sources. We show an example of an average stack at $3.6\mu\text{m}$ in Figure 1 and Table 1 summarizes stacking results for all IRAC wavelengths between $3.6\mu\text{m}$ and $8.0\mu\text{m}$. We obtained a strong detection of the stacked sources and the flat flux spectrum is consistent with the frequency spectrum of IR fluctuations that was found to be flat between $3.6\mu\text{m}$ and $8.0\mu\text{m}$ in Kashlinsky et al. (2007).

At these faint flux density values, the flux uncertainties are dominated by variations in the local background as well as the flux from the unmasked regions of nearby bright sources. To quantify this uncertainty, we also generated multiple stacks by offsetting the original ACS positions by random amounts, up to $\sim 9''$ from the original source coordinates. A stack was generated for each iteration and the stacked flux measured. The standard deviation of the flux values from each iteration provided the actual flux uncertainty quoted in Table 1. This uncertainty is significantly larger than the background shot noise by a factor of ~ 4 .

Based on the surface density of about 6000 galaxies in each GOODS field, we establish the absolute $3.6\text{ }\mu\text{m}$ IR intensity of these faint optical sources to be about $0.12\text{ nW m}^{-2}\text{ sr}^{-1}$. However, this estimate only accounts for sources that remain outside the IRAC mask and are not close to bright IRAC sources. Assuming the average flux from the stack also applies to sources affected by the mask, we estimate the absolute IRB intensity to be as high as $0.35\text{ nW m}^{-2}\text{ sr}^{-1}$. This is well within the range of 0.1 to $0.8\text{ nW m}^{-2}\text{ sr}^{-1}$ for faint sources below the individual point source detection level in existing deep IRAC images suggested with clustering models in Sullivan et al. (2007).

To further study the nature of these sources, beyond *Spitzer*/IRAC bands, we also stacked the same population at other wavelengths at which GOODS fields have imaging data. Specifically, for GOODS-N, we utilize the KPNO U-band (Capak et al. 2004), *Hubble*/ACS BV_{IZ} (Giavalisco et al. 2004), and near-infrared HK' (Capak et al. 2004). Similarly, for GOODS-S, we use the CTIO U-band and the ESO/ISAAC near-infrared data in the JHK bands in addition to the *Hubble* and *Spitzer* data. For the *Hubble* data, we simply stack the median flux values of the sources since they are mostly detected at all ACS wavelengths. It is almost impossible to stack images in the *Hubble* data because the galaxies have asymmetric morphologies at the spatial resolution of *Hubble*. For the other wavelengths, we excised subimages for each source and estimated a sigma clipped average of the subimages to obtain the stacked flux. Uncertainties were measured as described for $3.6\mu\text{m}$ data.

3. Redshift and Stellar Mass Density Estimates

In order to understand the physical properties of these faint galaxies, we fit the stacked flux in Table 1 with Bruzual & Charlot (2003; BC03) population synthesis models. Redshift, extinction, age, mass and e-folding time of star-formation were left as free parameters. For GOODS-S, which has better near-infrared data, we find a best fit redshift of 2.1, stellar mass of $1.3 \times 10^8\text{ M}_\odot$, $A_V=1.1$ mag, $t=15$ Myr, $\tau=100$ Myr (Figure 2) indicating an ongoing, reddened, starburst. The fit results in GOODS-N are very similar, with redshift of 2.6, stellar mass of $0.8 \times 10^8\text{ M}_\odot$, $A_V=0.4$ mag. The rest-frame 1500Å UV luminosity of the

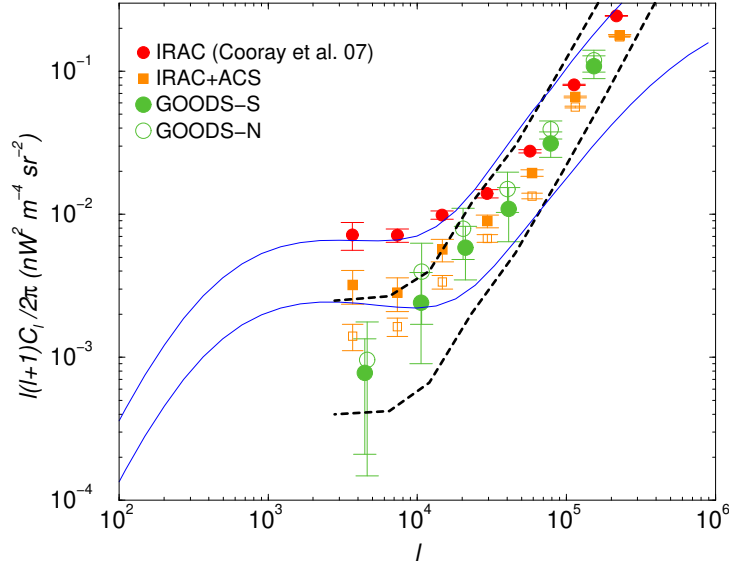


Fig. 3.— The top solid circles show the angular power spectrum of unresolved IR fluctuations in IRAC channel 1 ($3.6 \mu\text{m}$) of GOODS-N field. The solid squares show the angular power spectrum that masks the locations of faint ACS sources that are undetected in IRAC. The same power spectrum published in Cooray et al. 2007 is shown with open squares and the difference accounts for a new correction we have introduced here for the window function of the ACS source mask. With ACS sources masked, the fluctuation power spectrum amplitude is reduced at $\ell \sim 7 \times 10^3$ by a factor of about 2 (± 0.6). The circles and dashed lines below show the predicted power spectrum for faint optical sources with their $3.6 \mu\text{m}$ number counts distributed with two faint-end slopes: the open and filled circles are for clustering in GOODS-N and GOODS-S assuming the steeper slope for counts with $\alpha \sim 0.6$, while the dashed lines bracket the clustering for a flatter slope with $\alpha \sim 0$ ($dN/dm \propto m^\alpha$ when $m > 26$). For reference, the two solid lines are predictions from clustering models of the faint source population with the range covering the uncertainty in model parameters (Sullivan et al. 2007).

stacked galaxy is $1.8 \times 10^9 \text{ L}_\odot$ while its rest-frame V-band luminosity is $1.2 \times 10^9 \text{ L}_\odot$. Since $L_{*,\text{UV},z=3} = 5.8 \times 10^{10} \text{ L}_\odot$ and $L_{*,\text{V},z=3} = 8 \times 10^{10} \text{ L}_\odot$ (Steidel et al. 1999; Marchesini et al. 2007), it implies that these faint objects are galaxies which are about ~ 50 fainter than the characteristic luminosity of field galaxies at these redshifts.

Although the exact redshift distribution of these faint galaxies is not known at this time, it is illustrative to estimate the fraction of the stellar mass density hidden in these objects. We assume that the ~ 6000 galaxies that we have stacked on are distributed between $2.1 < z < 2.6$ with a stellar mass of 10^8 M_\odot . This corresponds to a co-moving stellar mass

density of $2 \times 10^6 \text{ M}_\odot \text{ Mpc}^{-3}$ which is a strong lower limit. Assuming that our stacked flux is typical for the ~ 22000 ACS sources which are unmatched to IRAC sources, would imply a total stellar mass density in faint galaxies of $6.7 \times 10^6 \text{ M}_\odot \text{ Mpc}^{-3}$ at $z \sim 2.4$. For comparison, the stellar mass density in Lyman-break galaxies at these redshifts is $3.6 \times 10^7 \text{ M}_\odot \text{ Mpc}^{-3}$ (Dickinson et al. 2003). Thus, faint, sub- L_* galaxies account for upto 20% of the total stellar mass density at $z \sim 2.4$.

4. Expected Clustering

We also measure the clustering of these sources to establish the amplitude of unresolved fluctuations at IRAC bands. Since we are interested in the anisotropy of IR light, to establish the power spectrum of fluctuations, we need the flux distribution within this population. The stacking analysis only allows us to establish either the total or the average flux of this sample. This forces us to make an estimate of the flux distribution and use that to predict clustering of unresolved fluctuations produced by these sources. The angular power spectrum of IR fluxes associated with these sources is determined using the same technique as described in Sullivan et al. (2007). We account for the flux distribution by randomly assigning IR flux to ~ 6000 source locations between 70 nJy and 700 nJy such that the total flux assigned is same as the total flux measured for these sources from the stack. We assign fluxes such that the number counts trace the extrapolated slope from known IRAC counts down to $m_{\text{AB}}(3.6\mu\text{m})$ of 24.7. Given the uncertainty in the faint-end slope, we take the slope α ($dN/dm \propto m^\alpha$) to be either 0.6 or 0.0. We tested how our predictions change with variations to these parameters and found consistent results within errors. Since the flux assignment is random, to get an average of the expected clustering, we randomize the assignments and the fluxes and use a Monte-Carlo approach to obtain the mean and variance of clustering.

We summarize our results in Figure 3, where we also compare with a direct measurement of the clustering of IR fluctuations and expectations based on the clustering models of Sullivan et al. (2007; solid lines). In Figure 3, we also show the IR fluctuation spectrum when the faint optical sources that we stack on are masked from the IRAC image with open squares (Cooray et al. 2007). The solid squares show the revised measurement after correcting for a bias associated with the window function introduced by the large mask. To understand this correction noted in Kashlinsky et al. (2007), we note that the fluctuation spectrum measurable in Fourier (multipole) space in the presence of a mask is $\hat{C}_\ell = \sum_{\ell'} W_{\ell\ell'} C_{\ell'}$, where $W_{\ell\ell'}$ is the window function associated with the mask and $C_{\ell'}$ is the power spectrum of interest. We recover the latter with measurements of \hat{C}_ℓ by first generating $W_{\ell\ell'}$ associated with our mask (Appendix A of Hivon et al. 2002) and then iteratively inverting for $C_{\ell'}$ using an inver-

sion similar to Dodelson & Gaztañaga (2000). The inversion agrees to 10% with a separate estimate of the angular power spectrum using a likelihood method where one maximizes the likelihood of an estimated C_ℓ^{est} with a model spectrum C_ℓ^{inp} using $C_\ell^{\text{est}} = \sum_{\ell'} W_{\ell'} C_{\ell'}^{\text{inp}}$ given the measurements \hat{C}_ℓ and the error σ_ℓ . This procedure can be described as minimizing the χ^2 with $\chi^2 = (\hat{C}_\ell - C_\ell^{\text{est}})^2 / \sigma_\ell^2$.

As shown in Figure 3, the difference between the fluctuation amplitude of unresolved IR fluctuations and the fluctuation amplitude with ACS sources masked is about a factor of 2 (± 0.6) at $\ell \sim 7 \times 10^3$. Our measurements then suggest that, from this difference, up to 50% of IR fluctuations can be accounted by faint ACS sources. It could be that by accounting for further fainter optically sources, this fraction can be increased, but it is unlikely that 100% of IR fluctuations first reported in Kashlinsky et al. (2005) are generated by $z > 8$ galaxies that are optically invisible.

The difference between IR fluctuations with and without ACS sources masked must be reproduced by the clustering of IR light produced by the same ACS sources. With flux assignments based on the stacking analysis, we find that the difference is reproduced (though these indirect estimates of the expected clustering IR fluctuations produced by faint ACS sources are uncertain due to uncertainties in the flux distribution). We conclude that irrespective of whether we measure the power spectrum in the IRB fluctuations after masking optical sources or whether we measure the power spectrum of faint optical galaxies with an average flux based on our stacking analysis, we find that the power in faint ($z_{AB} \sim 27$ mag), $z \sim 2.5$, galaxies accounts for at least $\sim 30\text{--}50\%$ of the power in the IR background fluctuations on angular scales of $\sim 4'$, where the measurement is not strongly sensitive to cosmic variance.

5. Discussion

The Kashlinsky et al. (2007) interpretation for IR fluctuations involves $z > 8$ galaxies with an IR background intensity as high as $4 \text{ nW m}^{-2} \text{ sr}^{-1}$ at $3.6 \mu\text{m}$. This is a large intensity given that all resolved sources, so far, lead to an IR background intensity of about $6.6 \text{ nW m}^{-2} \text{ sr}^{-1}$ when $m_{AB}(3.6\mu\text{m}) < 27$ (Sullivan et al. 2007; Fazio et al. 2004). To avoid individual detections of a large number of $z > 8$ galaxies, such a high background intensity must then be hidden in a source population with a large surface density but with individual faint fluxes of around 10 nJy for each source. Given the large surface density of the population, pixel to pixel intensity variations are a small fraction of the total intensity produced by those sources.

The alternative explanation is that a reasonable fraction of fluctuations arises from a population of sources that have a low surface density but are just below the *Spitzer*/IRAC detection threshold. The results from the stacking analysis presented here and suggest that faint optical galaxies, with an average source flux of around 130 nJy at 3.6 μ m, contribute between \sim 30-50% of the power in the fluctuations on the largest angular scales that we are able to measure. The average IR absolute intensity produced by these sources is as high as 0.35 nW m $^{-2}$ sr $^{-1}$ at 3.6 μ m. These sub-L $_{\ast}$ galaxies also contribute upto 20% of the stellar mass density at $z \sim 2.5$ and can be described as a low luminosity version of well-studied Lyman-break galaxies.

While these sources do not fully explain all IR fluctuations measured with deep IRAC images, in Cooray et al. (2007), we placed a conservative upper limit that any contribution from $z > 8$ sources must have an absolute intensity less than about 0.6 nW m $^{-2}$ sr $^{-1}$. Beyond *Spitzer* IRAC, studies have also been conducted at lower near-IR wavelengths with NICMOS and, though limited by the small field-of-view of NICMOS, they also show that IR fluctuations at 1.6 and 1.25 μ m are more consistent with a $z < 8$ origin than a high redshift interpretation (Thompson et al. 2007a, 2007b). Beyond IR fluctuations, it will be useful to further study the nature of this population and the role it plays in galaxy formation and evolution.

Acknowledgments: We thank Mark Dickinson for helpful suggestions. We also acknowledge the contributions of various members of the GOODS team who are associated with key aspects of data processing and handling. This research was funded by NASA grant NNX07AG43G, NSF CAREER grant AST-0645427, award number 1310310 from Spitzer for Archival Research, and program number HST-AR-11241.01-A by NASA through a grant from the Space Telescope Science Institute, which is operated by the Association of Universities for Research in Astronomy, Incorporated, under NASA contract NAS5-26555.

REFERENCES

Aharonian, F. et al. 2006, *Nature*, 440, 1018

Babbedge, T. S. R., Rowan-Robinson, M., Vaccari, M. et al. 2006, *MNRAS*, 370, 1159

Bruzual, G., & Charlot, S., 2003, *MNRAS*, 344, 1000

Capak, P., et al., 2004, *AJ*, 127, 180

Cooray, A. & Sheth, R. 2002, *Phys. Rep.*, 372, 1

Cooray, A. et al. 2004, *ApJ*, 606, 611; erratum-*ibid.* 2005, *ApJ*, 622, 1363.

Cooray, A. & Yoshida, N. 2004, *MNRAS*, 351, L71

Cooray, A. et al. 2007, *ApJ*, 659, L91

Dickinson, M. et al. 2003, in *Proceedings of the ESO Workshop, The Mass of Galaxies at Low and High Redshifts*, eds. R. Bender & A. Renzini, p. 324 (astro-ph/0204213)

Dickinson, M. et al. 2003, *ApJ*, 587, 25

Dodelson, S. & Gaztañaga, E. 2000, *MNRAS*, 312, 774

Dwek, E., Arendt, R. & Krennrich, F. 2005, *ApJ*, 635, 784

Giavalisco, M. et al. 2004, *ApJL*, 600, 93

Fazio, C. G. et al. 2004, *ApJS*, 154, 39

Fernandez, E. & Komatsu, E. 2006, *ApJ*, 646, 703

Hauser, M.G. & Dwek, E. 2001, *ARA&A*, 39, 249

Hivon, E. et al. 2002, *ApJ*, 567, 2

Kashlinsky, A. et al. 2004, *ApJ*, 608, 1

Kashlinsky, A. et al. 2005, *Nature*, 438, 45

Kashlinsky, A. et al. 2007, *ApJ*, 666, L1

Madau, P. & Silk, J. 2005, *MNRAS*, 359, L37

Marchesini, D., et al. 2007, *ApJ*, 656, 42

Matsumoto, T. et al. 2005, *ApJ*, 626, 31

Salvaterra, R. & Ferrara, A. 2003, *MNRAS*, 339, 973

Santos, M. R., Bromm, V., & Kamionkowski, M. 2002, *MNRAS*, 336, 1082

Steidel, C. C., et al. 1999, *ApJ*, 519, 1

Sullivan, I. et al. 2007, *ApJ*, 657, 37

Thompson, R. et al. 2007a, *ApJ*, 657, 669

Thompson, R. et al. 2007b, ApJ, 666, 658

Wright, E. L. & Reese, E. D. 2000, ApJ, 545, 43